

Microstructure and wear resistance of laser cladding Fe-based coatings reinforced by in situ synthesized TiB_2+TiC

TIAN YINGLIANG, LI QINGTANG, QIAO HONG, FU HANGUANG*, LEI YONGPING

School of Materials Science and Engineering, Beijing University of Technology, Beijing 100124, P. R. China

A Fe-based composite coating reinforced by in situ synthesized TiB_2 and TiC particles was fabricated on Cr12MoV steel by using 6KW fiber laser cladding. The microstructure and the microhardness of the coating in profile across were investigated by means of X-ray diffraction, scanning electron microscopy (SEM), energy dispersive spectroscopy (EDS), transmission electron microscope (TEM) and a hardness tester. The abrasive wear resistance of coating was evaluated using a MLS-225 wet sand rubber wheel testing machine. The coating mainly consists of TiB_2 、 TiC 、 Fe_2B and $\alpha\text{-Fe}$. The grains are refined. There are no cracks and few stomas in the coating. Defect-free coating with metallurgical joint to the substrate was obtained. From the surface of cladding layer 0.8 mm the highest micro-hardness is up to HV920, obviously higher than that of the substrate. Due to the exhibits of TiB_2 and TiC phases, the laser clad coating has good wear resistance.

(Received July 21, 2014; accepted October 28, 2015)

Keywords: Laser cladding, In situ synthesized, Micro-hardness, Wear resistance

1. Introduction

Laser cladding is one of the most useful surface engineering technologies for its special advantages and is extensively used in surface modification of metallic materials. Up to now, most reinforced phases are directly added into coating materials, because the surface of the particles is not clean or is contaminated, cracks may propagate from the interface between ceramic particles and the metal matrix [1]. In the recent decade, a new method called in situ synthesized has been extensively studied to produce composite materials. It can avoid the interface problem such as crack and poor compatibility with substrate to some extent [2]. In recently, a new Fe-Cr-B wear-resistant alloy based on M_2B eutectic boride has been studied a lot [3, 4]. Study found that Fe-Cr-B alloy has good wear-resistant and thermal shock resistance [5, 6]. This research aims to prepare a Fe-based composite coating reinforced by in situ synthesized TiB_2 and TiC to improve wear resistance of Fe-based coating.

In situ synthesized TiB_2 and TiC accords to the reaction ($\text{B}_4\text{C}+3\text{Ti}=2\text{TiB}_2+\text{TiC}$) on a Cr12MoV steel substrate by laser cladding. TiB_2 has high hardness, high melting point, high elasticity modulus, high temperature stability and these can make the coating has good binding properties with substrate [7]. As another reinforcing phase, TiC has a lower density, a better wettability and a higher hardness [8].

2. Experimental

The substrate was Cr12MoV steel. The Compositions of the substrate were 1.45%C, 0.27%Si, 0.32%Mn, 0.014%S, 0.020%P, 12.18%Cr, 0.23%V, and 0.57%Mo. The rectangular specimens of 15mm × 20mm × 40mm were cut from alloy plate, and the clad surfaces were ground to a surface finish of $\text{Ra}=0.1\text{mm}$. Laser cladding was conducted with a 1070 nm wavelength fiber laser with a BTSF-2 powder feeding system and a coaxial nozzle. The laser output power is 1.2 KW, the laser beam scanning velocity was 4mm/s, the powder feeding rate was 15g/min. The powder mixtures of the coating alloy were prepared from ferrotitanium (30 wt.%Ti, 100um), boron carbide(99.6 wt.%, 100um) and self-fluxing Fe-based powder. The amount of ferrotitanium and boron carbide was 20 wt.% and the ratio according to the reaction $\text{B}_4\text{C}+3\text{Ti}=2\text{TiB}_2+\text{TiC}$. The compositions of Fe-based powder are as follows: 1.65%B, 1.50%Si, 15.00%Cr, 0.15%C, and the rest is Fe.

A Japan Shimadzu X-ray diffractometer (XRD) with $\text{Cu-K}\alpha$ radiation was used to analyze the phases of the coating. An S-3400N scanning electron microscope (SEM) coupled with an energy dispersive spectrometer (EDS) and a JEM-2100 transmission electron microscopy (TEM) were employed to characterize the microstructure. An MICRO MET-5103 hardness tester was used to measure the microhardness every 0.4mm from the surface, and the load was 4.9 N.

The abrasive wear resistance was evaluated using a MLS-225 wet sand rubber wheel testing machine. 60-80 meshed quartz sands mixed with water in a ratio of 1:3 were used as wet wear medium. The applied load was 200 N. The speed of rubber wheel was 240r/min and its hardness is 60 shore A. The weight loss of the test specimens was evaluated by an electronic analytical balance with a precision of 0.1mg. The results of wear tests were the average of three tests. The surface morphology of wear scar was examined by scanning electron microscope.

3. Results and discussion

3.1 Microstructure of coating

Fig. 1 shows a typical microstructure of the composite coating. We can see many particles with different sizes, whose diameter is from $2\mu\text{m}$ to $8\mu\text{m}$. In general, the distribution of particles is uniform in the matrix. The small-sized particles are commonly precipitated in three kinds of morphologies, such as quadrangle, cluster, and flower-like shape. The most large-sized particles are quadrangle and pentagon. The elemental compositions (in atom %) are as follows: Point A (41.34C, 54.57Ti, 4.09Fe), and Point B (18.32C, 33.59Ti, 0.42Fe, 47.39B, 0.28Cr). We can see that A region mainly contain C, Ti elements while B region mainly contain C, Ti, B elements. In A region the Ti/C atomic ratio is approximately 1/1. Finally, and according to XRD results, the A region can be identified as the TiC and B region as the mixture of TiC and TiB_2 . We can infer that portion TiB_2 phase nucleates on the surface of TiC particles or in their close vicinity as the large-sized particles mosaic the small ones.

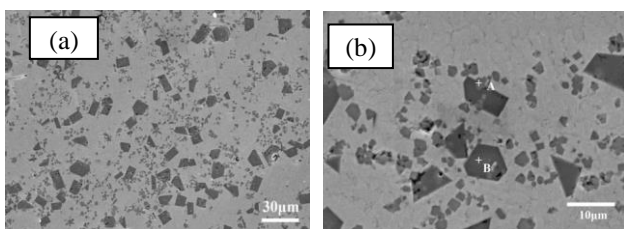


Fig. 1. SEM images of clad layer: (a) low magnification; (b) high magnification

3.2 XRD spectrum of coating

Fig. 2 shows the XRD spectrum of the coating layer. Owing to non-equilibrium effects of the rapid remelting and solidification in laser cladding resulted in an extension of saturation and distortion of the lattices, it was difficult to identify the phases present in the coating. However, by comparing and analyzing, it can be found that the cladding coating was mainly composed of $\alpha\text{-Fe}$, TiC, TiB_2 and Fe_2Ti , which means that the TiC and TiB_2 can be formed in-situ.

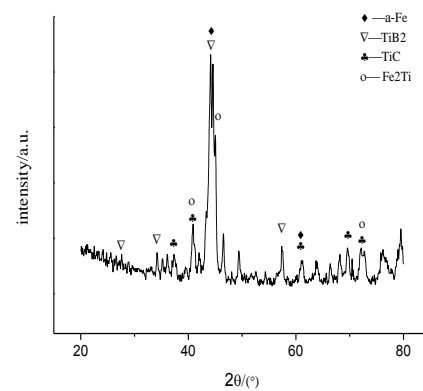


Fig. 2. XRD patterns of the clad layer

3.3 TEM

Fig. 3(a) shows a typical TEM micrograph of TiC particles in the coating and EDS analysis on point A is shown in Fig. 3(c). Its clearly demonstrate that point A is TiC. Fig. 3(b) is the selected area electron diffraction, which shows that the TiC has an fcc crystalline structure. From the Fig. 3(d) we can see a thin needle-shaped microstructure is formed by a martensitic transformation owing to the very rapid solidification rate.

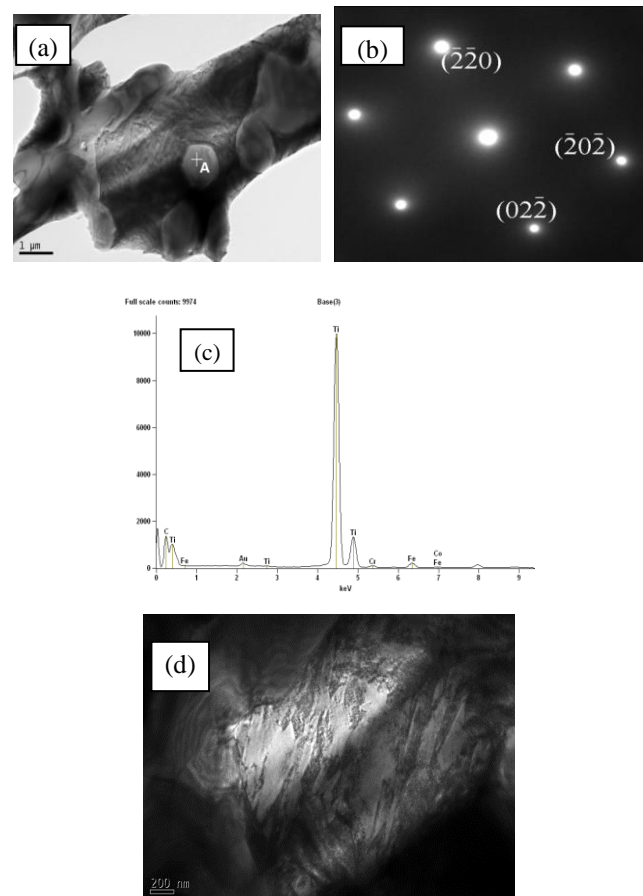


Fig. 3. TEM micrograph of TiC particles in the coating: (a) TiC morphology; (b) electron diffraction of TiC; (c) EDS analysis on point A; (d) martensitic structure

3.4 Microhardness

The microhardness profile along the depth direction of the coating is shown in Fig. 4. We test the hardness at intervals of every 0.4 mm, and then took the average measurements of five different points at the same depth. We can see the highest microhardness of the cladding layer is up to 920 HV, which is mainly attributed to the presence of reinforcements TiC and TiB₂. The theoretical hardness values of TiB₂ and TiC are about HV3400 and HV3000 [10]. The dispersive distribution of such high hardness reinforcements could cause the increase in hardness of the whole coating. What's more, fine grain structure from rapid melting and cooling under the laser cladding also promote the improvement of microhardness. We can see that the microhardness within the coating gradually increases from the bottom to the top surface of the coating and it ensured the highly mechanical properties. In addition, another reason for the high microhardness is owing to martensitic transformation. Because of solid phase transformation and the very rapid solidification rate, thin needle-shaped microstructure is formed by a martensitic transformation.

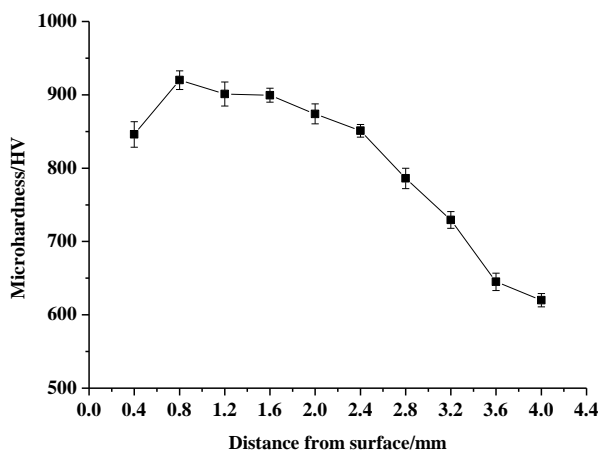


Fig. 4. The microhardness of clad layer

3.5 Wear resistance

As for the sample, block-like specimen (10 × 25 × 57 mm in size) was fixed on the MLS-225 wet sand rubber wheel testing machine was pressed under applied loads of 200N. We used silica sand less than 0.4 mm for abrasive. During sliding, the speed of rubber wheel was 240 r/min, it rings with 176 mm in outer diameter and the hardness was 60 shore A. The wear mass loss of the samples was determined by an electronic analytical balance with an accuracy of 0.1 mg. To ensure the accuracy of measurement, the specimen was cleaned for 10 minutes before measurement.

In comparison with the Cr12MoV steel, the laser clad coating exhibits good wear resistance, as indicated in Fig. 5. Wear mass loss of the coating is nearly 1/2 of that of the Cr12MoV steel. From Fig. 6(a) we can see plastic deformation and deep plowing grooves on the worn surface and were mainly abrasive wear and adhesion wear. TiC and TiB₂ reinforcements make an important role in resisting the abrasive wear and adhesion wear in the process of the sliding owing to their high hardness. During the course of friction, reinforcements have the pinning effect and then hinder the plastic deformation of the matrix. Because of their strengthen action, the loss of laser cladding material and its wear resistance get evidently improved. The TiC and TiB₂ hard phases are relatively protruding on the friction surface [9]. As they can first slowly be consumed by micro-cutting and scratching, the wear morphology of cladding layer is bright at these sites, as can be seen in Fig. 6(b). From Fig. 7(a) we can see some peeling pits in different sizes. This is about the break off of hard phase particles. In the initial stage of friction process, wear occurs on the low hardness and poor abrasion phases, but over time, hardness phases beset in the cladding layer protrude on the friction surface and then act as supporting load limiting the direct contact between wheel and layer. After repeat friction, the hard phase fatigue and its size decrease and the adhesion with layer metal declines. Fig. 7(b) shows this clearly, we can see a bright girdle between grain boundaries and layer metal. It is so obvious that seemed to shine in the darkness. The grains fall off when friction to a certain extent. This period, the wear mechanism of coatings appeared to be obvious fatigue wear.

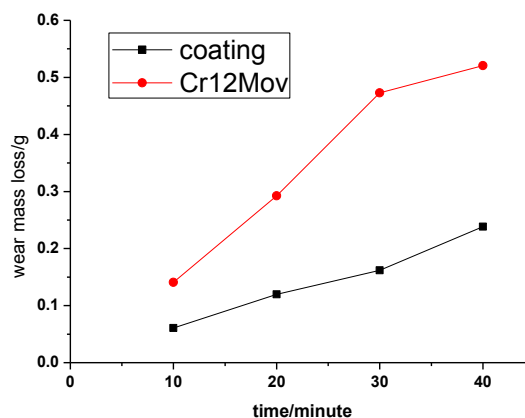


Fig. 5. Wear mass loss of laser cladding coating and Cr12MoV steel.

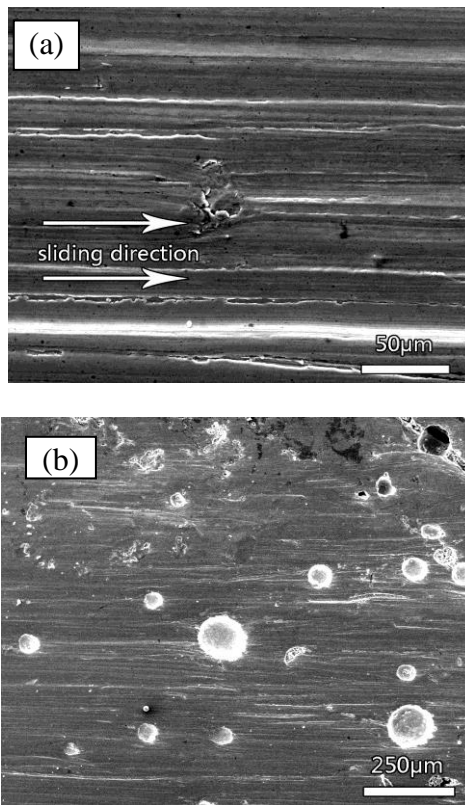


Fig. 6. SEM images showing worn surface morphologies of laser clad coating. a) low magnification); b) high magnification.

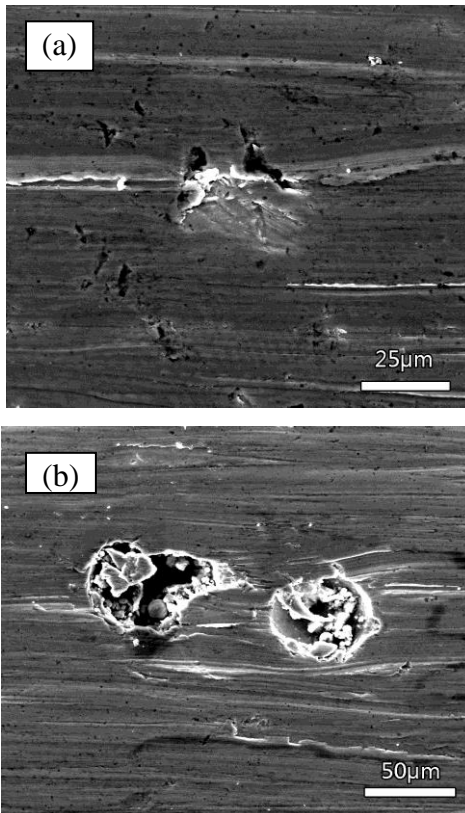
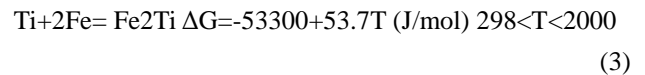
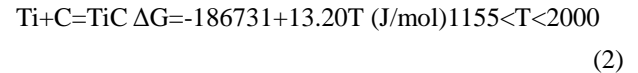
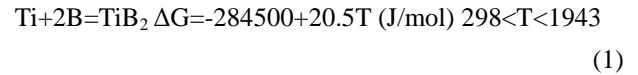


Fig. 7. SEM images showing wear debris morphology. a) low magnification); b) high magnification

4. Generating mechanism analysis

Various chemical reactions may occur in the coating and formed new compounds during the process of laser cladding. The main reactions between C, Ti, B, Fe are considered and Gibbs free energy of these reactions were as follows:



These formulas demonstrate that TiC and TiB₂ reinforcements can be in situ synthesized in the coating. From the Fig. 1a we can see that reinforcements distributed on the substrate with different size and different morphology. There is black spots mosaic in the large precipitates and EDS analysis show the black spots mainly contain TiC and TiB₂. When the concentration fluctuation, energy fluctuation and structure fluctuation to a certain extent, which can meet the desired nucleation of TiC in the Fe-based cladding layer, TiC begin to nucleation and growth. During this process Ti, C atoms are observed and at the same time B, Fe atoms could be ejected. Along with growing of TiC, the concentration of B is increased and resulted in heteroepitaxy growth of TiB₂ on the surface of TiC. In the meantime, some precipitates are formed during the solidification, this precipitates get small size as the diffusion rate restrict its growing. The involved in situ-synthesized reactions are all exothermic reaction, whose liberated heat combined with laser can make parts of the reinforcements remelting then formed Fe-Ti-B-C melt.

5. Conclusions

(1) A Fe-based composite coating reinforced by in situ synthesized TiB₂ and TiC particles was fabricated on Cr12MoV steel by using 6KW fiber laser cladding. The coating mainly consists of TiB₂, TiC, Fe₂B and α -Fe.

(2) From the surface of cladding layer 0.8 mm the highest microhardness is up to HV920, obviously higher than that of the substrate. The high hardness of cladding layer is owing to the presence of reinforcements TiB₂ and TiC, martensitic transformation and fine grain structure from rapid melting and cooling.

(3) Due to the exhibits of TiB₂ and TiC phases the laser clad coating has good wear resistance. The wear mechanism of coatings appeared to be abrasive wear, adhesion wear and fatigue wear.

Acknowledgments

The authors would like to thank the financial support for this work from National Natural Science Foundation of China under grant (51475005), Natural Science Foundation of Beijing under grant (2142009), Scientific Plan Item of Beijing Education Committee under grant (PXM2015-014204-500170).

References

- [1] Li Jun, Zhang Xuanjun, Wang, Huiping, Li Manping, International Journal of Minerals, Metallurgy and Materials, **20**(1), 57 (2013).
- [2] Yang Sen, Liu Wenjin, Zhong Minlin, Wang Zhanjie, Kokawa Hiroyuki, Journal of Materials Science, **40**(9-10), 2751 (2005).
- [3] Du Baoshuai, Li Qingming, Wang Xinhong, Zou Zengda, Transactions of the China Welding Institution, **28**(4), 65 (2007).
- [4] H. Zhang, H. Fu, Y. Jiang, H. Guo, Y. Lei, R. Zhou, Q. Cen, Materialwissenschaft und Werkstofftechnik, **42**(8), 765 (2011).
- [5] P. Christodoulou, N. Calos, Materials Science and Engineering A, **301**(2), 103 (2001).
- [6] Guo Changqing, P. M. Kelly, Materials Science and Engineering A, **352**(1-2), 40 (2003).
- [7] Li Jun, Zhang Huiying, Li Wenge, Zhang Guangjun, Rare Metals, **27**(5), 451 (2008).
- [8] Wang Xinhong, Zhang Min, Zou Zengda, Qu Shiyao, Surface and Coatings Technology, **161**(2-3), 195 (2002).
- [9] Yang Maosheng, Liu Xiubo, Fan Jiwei, He Xiangming, Shi Shihong, Fu Geyan, Wang Mingdi, Chen Shufa, Applied Surface Science, **258**(8), 3757 (2012).
- [10] Fu Hanguang, Beijing: Machinery Industry Press, 2011.

*Corresponding author: hgfu@bjut.edu.cn